Preparation and Evaluation of Epoxy-Clay Nanocomposite Coatings for Corrosion Protection

D. Zaarei, A. A. Sarabi*, F. Sharif, S. M. Kassiriha, M. Moazzami Gudarzi

Polymer Faculty, Amirkabir University of Technology, Tehran, I. R. Iran

(*) Corresponding author: sarabi@aut.ac.ir
(Received: 28 Jan. 2010 and Accepted: 31 May 2010)

Abstract:
Polymer-clay nanocomposite coatings have attracted much attention because of impressive enhancements of coating properties. In this research, both commercially available and isophoronediamine-modified montmorillonite clays were used to obtain epoxy-clay nanocomposite coatings. These nanocomposite materials with different clay loadings in the form of coatings were applied to cold-rolled steel (CRS).The morphology and structure of the coating compositions were characterized using sedimentation tests of X-ray diffraction (XRD) and transmission electron microscopy (TEM). The corrosion resistance properties of the neat resin and nanocomposite coatings in 3.5% NaCl solution were investigated by electrochemical impedance spectroscopy (EIS) for more than 210 days. After making the measurements, we found advanced protection of nanocomposite samples against corrosion compared with the neat resin. Also, the results showed that the dispersion quality of clay layers into the matrix depended on the structure and modification of clay and the compounding method. Coating compositions containing two or more weight percent of well-dispersed clay resulted in superior corrosion protection. Considering the structure and compounding methods, corrosion protection of both nanocomposite coatings containing amine-modified and commercially available clays was excellent.
Keywords: *Nanocomposites, Epoxy, Morphology, dispersion, electrochemical impedance spectroscopy*

1. INTRODUCTION

Some of the most effective anticorrosive undercoatings based on chromium-containing compounds may need to be replaced with alternative materials due to the environmental and health concerns [1-7]. Since 2007, the strict Environmental Pollution Agency (EPA) regulations have required elimination of the heavily used chromate inhibitors [8]. Therefore, it is a long time some environmental friendly and effective corrosion inhibitive coatings applicable to different industries, were investigated.

Nanoscale materials may have unique physical, chemical and physicochemical properties to allow for improvements in corrosion protection compared with bulk size objects made of the same materials. It has also been well-known that such nanoparticles create high surface area to allow their uniform dispersion into matrix materials with a low dosage so that the efficiency of nanocomposites could be significantly enhanced in terms of materials properties [9].

Recently, organic–inorganic nanocomposites have attracted considerable attention because of their remarkable properties and unique structure which

has led to the synthesis and study of a large number of these hybrid composite materials [10]. The intercalation of organic guest-species into inorganic materials is a way to construct an ordered organic–inorganic assembly [11]. Polymer intercalated nanocomposites prepared by using layered materials are expected to lead to a high degree of polymer ordering and exhibit advanced gas barrier, thermal stability and enhanced mechanical properties compared with pristine polymers [12-13]. Based on these properties, nanocomposites differ from traditional composites and lead to a complex interaction of the nanostructural heterogeneous phases. In addition, nanoscopic particles differ greatly in the analogous properties from a macroscopic sample of the same materials. Making use of the desirable properties of both materials, the combination of organic and inorganic materials, offers novel properties due to the synergistic effect of both components [14-15].

Many researches have been done to integrate inorganic nanolayers like montmorillonite (MMt) clay into the organic polymeric matrices. It has been found that the incorporation of inorganic nanolayers of MMt clay into the polymeric matrix can effectively enhance the corrosion protection effect of pristine polymers such as conducting polymers (e.g., polyaniline, poly (o-methoxyaniline), poly (O-ethoxyaniline), poly (3-alkylthiophene), polypyrrole, thermoplastic polymers (e.g., poly (methyl methacrylate), and thermosetting polymers (e.g., polyimide) on cold-rolled steel (CRS) coupons based on a series of electrochemical corrosion measurements in saline [16]. These materials with a plate-like shape are usually employed to effectively increase the length of the diffusion pathways for oxygen and water as well as decrease the permeability and corrosion receptivity of coatings [7].

In the present study, two types of commercially modified MMt with different loadings were introduced into an epoxy matrix. A cycloaliphatic amine was used as a raw clay modifier and the modified clay was introduced into the epoxy matrix via slurry compounding [17-19]. The morphology and structure of the resultant nanocomposites were characterized by fourier transform infrared spectroscopy (FTIR), X-ray, TEM tests. The protective properties of the neat resin and nanocomposite coatings were evaluated by electrochemical impedance spectroscopy (EIS). The difference among three types of nanocomposite coatings and the role of clay dispersion in corrosion inhibitive properties were studied. Moreover, the effects of the clay content on the corrosion resistance of resultant coatings were evaluated.

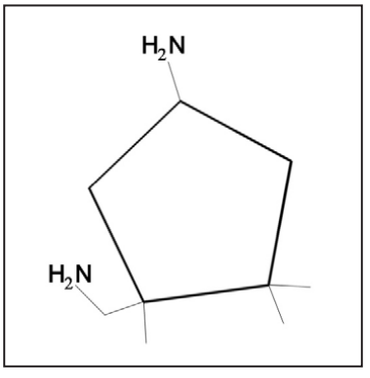

Figure 1: *Chemical structure of (3-(aminomethyl)-3,5,5-trimethylcyclohexan-1-amine)(IPDA) as modifier of clay and curing agent*

2- EXPERIMENTAL

2.1. Materials

The epoxy resin used was an aromatic one, diglycidylether of bisphenol A (DGEBA) in the form of Epon 828 supplied by Shell Chemicals. The epoxide equivalent weight and viscosity of the resin were about 178-190 g. and 11-15 Pa.s at 25°C, respectively. 3-(aminomethyl)-3, 5, 5-trimethylcyclohexan-1-amine or Isophoronediamine (IPDA), which was used for curing the resin were purchased from Sigma-Aldrich, (Singapore). Two different types of commercially modified clay were used. The first one was Cloisite 30B (C30B) supplied by Southern Clay Products. This material was methyl tallow bis (2-hydroxyethyl) quaternary ammonium ion-modified MMt with cation exchange capacity (CEC) of 90-95 meq/100 g. The other one was Nanomer I.30E (I.30E) from Nanocor Inc. The modifier of this material was octadecyl ammonium ion-modified MMt with CEC of 145 meq/100 g [20].

Unmodified sodium MMt, Cloisite Na (CNa), was obtained from Southern Clay Products with CEC of 90-95 meq/100g. The chemical structure of IPDA is shown in Figure 1. Other materials such as ethanol, hydrochloric acid (HCl) and silver nitrate ($AgNO_3$) were purchased from Merck.

2.2. Clay modification

Five grams of CNa was gradually suspended in 200 ml of distilled water and stirred vigorously by a magnet stirrer for 30 min at ambient temperature in a three-necked flask. In a separate beaker, 0.667 gr. of concentrated hydrochloride acid (37%) was added to 50 ml ethanol and then 1.142 gr of IPDA was added to that beaker. The molar ratio of IPDA to HCl in the mixture was less than one to protonate only one amine function of IPDA. This mixture was stirred for 5 min and then added to the clay suspension. The reaction mixture was stirred for 2 hr under the reflux (90-95ºC). A white precipitate was formed, which was isolated by centrifuging and washed several times with hot water until no chloride ions were detected in the filtrate by one drop of 0.1 N of $AgNO_3$ (aq.) solution. The water in the suspension was removed by centrifuging and washing with acetone for several times. This clay was named Clay Modified with IDPA (CIP). CIP-acetone slurry was used for preparing nanocomposites. For the XRD and FTIR studies, some of the suspension was poured into the Petri dish and dried in an oven at 110ºC for 5 hr.

2.3. Epoxy-clay nanocomposite preparation

The remainder of the above CIP-acetone slurry was added to the desired amount of epoxy resin and sonicated with a high-powered sonication instrument (UP400 made by Heischler Company) for 10 min. To remove the eventually remaining residual acetone, the mixture was put in an oven at 80ºC for 30 min. The obtained mixture was sonicated for another 10 min. Part of this uncured mixture was separated for XRD analyses. For the curing of this nanocomposite, a stoichiometric amount of the hardener (IPDA) was added and thoroughly mixed. The weight ratio of base/hardener was 100:23.

On the other hand, conventional nanocomposites were prepared using two commercial organoclays, that is, I.30E and C30B. Epoxy resin was slowly heated up to 50ºC and an appropriate amount of clay was gradually poured into the resin during stirring. The mixture was held at 70-80ºC and stirred at 2500 rpm for 2.5 hr with a high-shear mixer. Then the samples were degassed in a vacuum oven at 80-85ºC for 30 min. These mixed compositions containing resin and clays were sonicated for 120 min. A stoichiometric amount of the hardener (100:23) was added and the composition was thoroughly mixed. Afterwards, the mixture was stirred for 3 minutes and sonicated for 2 minutes. The code and composition of different coatings are shown in Table 1.

The coating compositions were degassed and applied to the surface of the pretreated cold-rolled steel (CRS) plates with a film applicator. The pretreatment process of CRS plates was the emery cloth sanding and solvent (acetone/ethanol 2:1) cleaning. The dimension and roughness (Rz) of the steel plates was 150*60*1mm and 3µm, respectively. The thickness of the nanocomposite coating films was 27±3 µm. The coating films were post-cured in an oven for 1 hr in 100°C.

Table 1: *Code and composition of prepared coatings*

Composition code	Wt % Clay in coating composition	Type of clay
NR	0	-
1C	1	Cloisite 30B
2C	2	Cloisite 30B
3C	3	Cloisite 30B
4C	4	Cloisite 30B
2I.30E	2	NANOMER I.30E
2CIP	2	Cloisite Na (modified with Isophoronediamine)

2.4. Characterization

Sedimentation was visually observed for the uncured compositions of the clay and resin held at 135˚C for nearly 25 min [21].

The degree of interlayer distance of the clay layers in the fully cured nanocomposite samples was determined by XRD. These analyses were performed using a Philips analyzer model PW 1840 with CuKα radiation (λ=1.5401 Å) operating at 40 kV and 30 mA. The diffraction patterns were obtained from 2θ range of 1° to 10° at the rate of 0.01°/min and the step size was 0.02. the CNa, CIP, C30B and I.30E powders were analysed by XRD.

For TEM tests specimens were cut off the nanocomposite blocks using an ultra microtome, OMU3 (Reichert, Austria) equipped with a diamond knife. Thin specimens (70–100 nm) were also cut from a mesa of about 1*1 mm^2. The samples were placed on 300 mesh copper grids. Transmission electron micrographs were taken with a Philips-CM200 at an acceleration voltage of 200 kV.

Infrared spectra of the samples were measured with a FT-IR spectroscopy (Digital Vector 33, Bruker) using KBr pellets. Scans were operated from 400 to 4000 cm^{-1} and took 40 sec to complete. To investigate the effect of modification on CNa, the chemical structures of IPDA as a modifier and those of CNa and CIP were acquired.

For the EIS measurements, a three-electrode cell was used: the working electrode with an exposed area of 1 cm^2 of coated CRS plates, an Ag/AgCl reference electrode with 3M solution of KCl and a platinum auxiliary electrode. The corrosive medium was a 3.5 wt% of NaCl solution at ambient temperature. Other areas of working electrodes were sealed with 2.5:1 mixture of beeswax–colophony. The EIS measurements were performed using an Autolab G12 (Italy). The measurements were carried out for 320 days of immersion at open circuit potential at a frequency range of 10^{-2}–10^4 Hz with 10 mV perturbations. EIS data were analyzed by Frequently Response Analyzer (FRA) software version 4.9.005 (Autolab, Italy). The experiments were conducted in triplicate.

3. RESULTS AND DISCUSSIONS

3.1. Substitution of diamine inside the clay galleries

The evidence for the reaction between the ammonium group of IPDA salt and CNa platelets via cation exchange comes from FTIR studies. FTIR spectrum of the pristine clay (CNa), IPDA, and CIP is shown in Figure 2.

The FTIR spectrum of CNa was compared with that of CIP and IPDA. The presence of 3628 cm^{-1} peak in the spectrum of pristine clay can be attributed to –OH stretching. Significant characteristic peaks of water (3448 cm^{-1}, 1640 cm^{-1}) can be seen in Figure 2. The occurrence of ion exchange reaction between IPDA ammonium salt and pristine clay (CNa) can

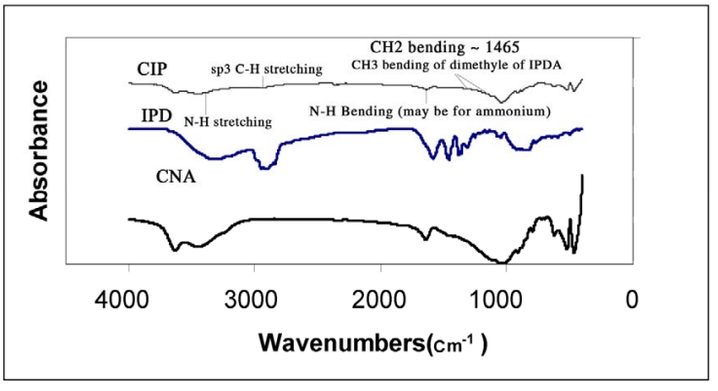

Figure 2: *FTIR spectra of IPDA, CNa and CIP*

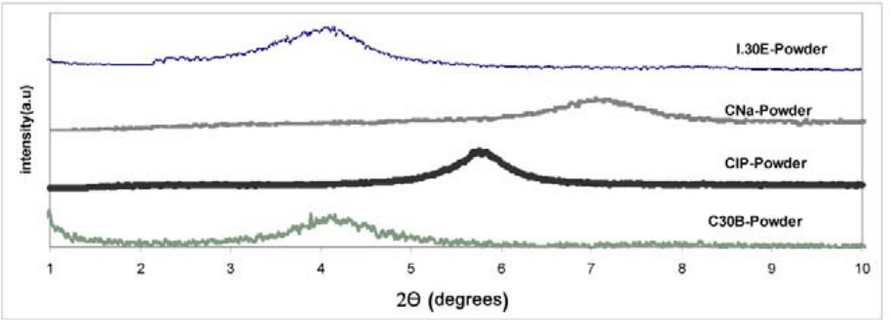

Figure 3: *XRD patterns of C30B, CNa, I.30E and CIP powders*

be confirmed by the appearance of some new peaks in the CIP spectrum. The spectrum of CIP displays some new peaks in 1360-1380 cm^{-1}, 1520 cm^{-1} and 2900-2950 cm^{-1} which indicate $–CH_2$ bending, N-H bending in ammonium and sp^3 C-H stretching.

Figure 3 shows the XRD patterns of C30B, I.30E and CIP powders. Based on the Braggs law, the d_{001} of C30B, I.30E, CNa, and CIP were 18.02Å, 21.66Å, 12.27 Å and 15.36 Å, respectively. These results indicate the opening between the silicate sheets in terms of the basal interplanar spacing of CNa, C30B as well as CIP. The increment of d-spacing of CIP clay caused by our method was 3.09 Å, while the increment of d-spacing for commercially modified C30B was 5.75Å. In other words, the IPDA molecules were introduced to and penetrated between the clay layers. So, the intercalation in the CIP, like the C30B has occurred.

3.2. Dispersion and Structure

The results of sedimentation test showed no settlement when C30B organoclay was used in compositions prepared with high-shear mixing plus sonication methods. Similarly, there was no settlement when CIP organoclay was used in compositions prepared by amine modification plus slurry compounding method. On the other hand, some relatively large I.30E clay particles have presumably settled after using high-shear mixing plus sonication. That is, the high-shear mixing followed by sonication did not exert enough shearing force for the dispersion of I.30E clay particles.

It can also be suggested that the settlement was a function of organophilicity as well as cation exchange capacity (CEC) and clay compounding method. The findings, moreover, show better dispersion and better compatibility of C30B and CIP clays with epoxy resin. This maybe due to the lower affinity of the organic modifier I.30E to the epoxy resin. In the dispersion process, slurry compounding increased the rate of diffusion of the epoxy monomers into the galleries and broke the whole stacks of clay to smaller particles [17, 22-24].

However, better dispersion means that there is no gradient in the concentration of clay layers. On the other hand, some clay layers could be exfoliated but the dispersion of these individual layers at the matrix may not be homogeneous [25]. In the dispersion process, the cluster of stacks must be broken down to the tactoids homogeneously. Perfect dispersion is a difficult task so, many researches are being carried out in this area [26-27]. In our pervious work, we found that the mechanical mixing could not provide enough energy to disperse particles; therefore, some agglomerates remained in the matrix [23]. The ultrasonic mixing technique can reduce the size of particles and disperse them homogeneously if the compatibility between clay surfaces and the matrix was adequate. So, ultrarasonication would be a useful technique if the nanoscale dispersion in a thermodynamic way was possible [23].

Figure 4 presents the X-ray diffraction patterns of cured nanocomposites prepared with 2I.30E, 2C as well as 2CIP clays. These patterns corresponded to the interlamellar spacing of the clay. No peaks were detected for the CIP nanocomposite in the range of 2θ from 1° to 10°. The XRD patterns of nanocompoites containing C30B show a low intensity peak 2θ around 2.5° that reveals the presence of an ordered structure.

Furthermore, an opening between the silicate sheets in terms of basal interplanar spacing of organomodified MMt was observed. A single and relatively large peak was found for I.30E containing nanocomposites. This means that the high-shear stirring and sonication method could not afford enough shearing force for the dispersion of I.30E clays; therefore, a further step was taken to achieve a uniform composition. The patterns of CIP reflected the amorphous halo of the nanocomposite materials. However, the absence of peaks in 2CIP in this range may imply that the distance between the clay layers in the epoxy was too large to be detected by X-ray analysis. It seems likely that the main reason behind these observations was the elastic forces which applied to the silicate layers from the polymer network during the curing process [25, 28].

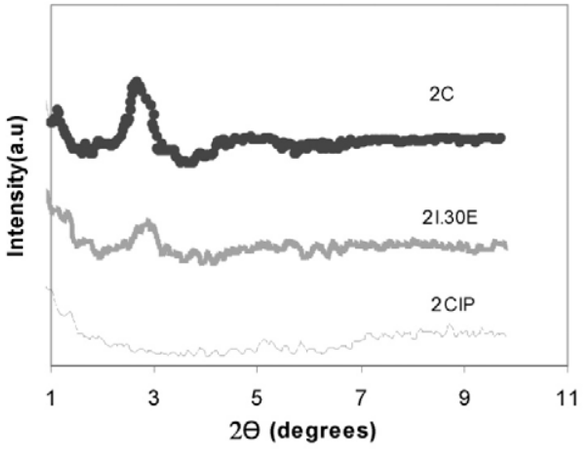

Figure 4: *XRD patterns of cured epoxy-clay nanocomposites Containing 2 wt% of C30B, I.30E and CIP*

The state of exfoliation and intercalation inferred from XRD was further analyzed by TEM. The transmission electron micrograph of nanocomposites containing 2wt % of CIP and C30B clays is shown in Figure 5. Because of the existence of some relatively large I.30E clay particles settled after the dispersion process, we could not achieve the uniform composition of this material, so the TEM images of nanocomposites containing this clay were not attainable.

Individual crystallites of the silicate were visible as regions of alternating narrow, dark and light bands within the particles. Figure 5(b) shows the nanocomposites containing 2Wt% of CIP clay which was prepared with slurry compounding. Figure 5(a) shows nanocomposites containing 2Wt% of C30B clay. The separations were from 2 to 9 nm indicating intercalation of clay layers [29]. The variable thickness was due to the stack of silicate layers one above the other, thus indicating that even in a well-dispersed nanocomposite, significant layer stacking has occurred. These figures show separations in the CIP nanocomposites with more than 9 nm, indicating exfoliated dispersion. Therefore, the mechanical stirring and the ultrasonic separation techniques could not be effectively used to fully separate the agglomerations of the nanoclays.

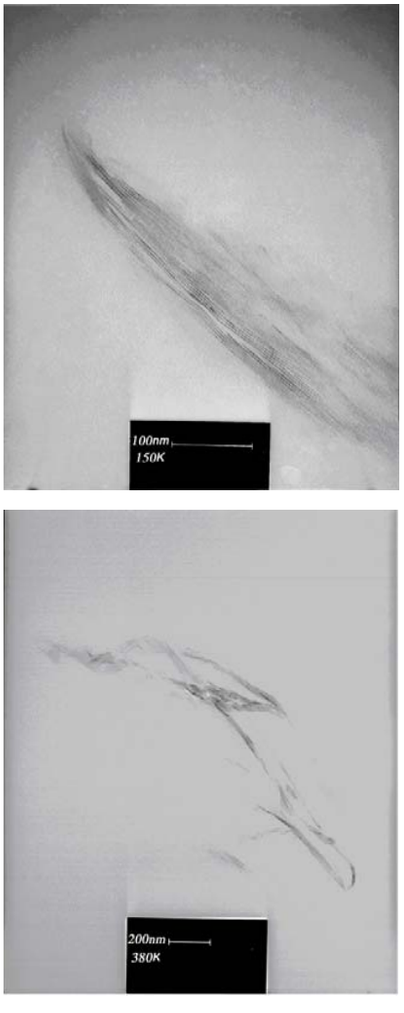

Figure 5: *TEM images of cured epoxy-clay nanocomposites : a) 2C, b) 2CIP*

The platelet spacing indicated by TEM images confirms by XRD results. However, these results affirm that the type of the processing and the type of the modifiers of clay lead to the previously mentioned morphologies. The IPDA modification of the clay via the slurry compounding allows it to be more easily dispersed and exfoliated under our experimental conditions in the specific quantities of organoclay loading. It can be concluded that the presence of the reactive groups on the surface of clay leads to intercalation of galleries as shown in XRD patterns of uncured compositions.

In CIP systems, polymerization rate in the galleries was large enough because high- acidity primary amine (IPDA) was used as surfactant. It could be predicted that this cation has the catalytic effect on the curing because of the higher value of its acidity. This is a desirable effect because not only the exfoliation improves, but also better dispersion is achieved due to the type of compounding as well as high compatibility of these molecules with the matrix as discussed above.

3.3. Corrosion resistance of different coatings

For the organic coatings, the usual interpretation of the impedance diagrams is that the high-frequency part is related to the organic coating while the low-frequency part corresponds to the reactions occurring on the metal through defects and pores in the coating [30-31]. The impedance at the frequency of 0.01 Hz (Log $|Z|_{0.01}$), is usually used as an indication of polarization resistance. The impedance diagrams were plotted to characterize the corrosion resistance of the CRS substrates covered by NR, 2CIP, 2I.30E, 2C, 3C and 4C. The impedance at the frequency of 0.01 Hz (Log $|Z|_{0.01}$), as Bode modulus, was plotted after six different exposure times in the 3.5 wt% NaCl solution. These plots are presented in Figures 6.

As shown in Figure 6., NR coating exhibited relatively high resistance during the initial stages of immersion, with the impedance value in low frequency reaching to more than approximately 10^9 orders of magnitude. $|Z|_{0.01}$ for NR decreased with increasing the immersion time, and corrosion resistance decreased during the first 30 days of immersion, which indicates a loss of the barrier properties of the coating film. Figure 7 shows that the $|Z|_{0.01}$ for 1C and 2I.30E decreased with increasing the immersion time. The fall of $|Z|_{0.01}$ during the few days of exposure was attributed to the penetration of the electrolyte through the coating. As a matter of fact, the $|Z|_{0.01}$ values for 1C and 2.I30E remained orders of magnitude higher than that for NR. For the NR coating, the impedance value was decreased to lower than 10^6 after 150 days of immersion. At this time, black spots of rusting could be observed on the surface of CRS substrate**.** Figure 6 also indicates that the incorporation of a low amount (1C) of clay compared with NR, positively affected the corrosion resistance of the resultant coating.

EIS was also performed on 2CIP, 2C and 4C coating systems. Figure 7 shows that the resulting Log $|Z|_{0.01}$ in these coatings were much higher than that of NR, 1C and 2I.30E, in different periods of exposure in NaCl solution. It must be noted that the thickness of the both coatings was the same.

As shown in Figure 7., $|Z|_{0.01}$ of the epoxy coating without any clay (NR) is much lower than that for the other coating systems after 210 days of immersion. On the other hand, 2C, 3C, 4C and 2CIP coating systems show apparently better performance than the other systems, indicating that the dispersed clay layers can effectively block the pores formed in the coating film. Although the corrosion resistance of 2I.30E was better than that of NR, its performance was poor, in comparison with 2C and 2CIP.

For small nanoparticles, free space between the particles and the resin was far less than that of larger particles. Thus, the electrolyte was harder to penetrate through the pores in coating film which contained nano-sized pigments [32]. In addition, due to longer diffusion path around the clay in the high clay loading films, the water and ions need more time to reach to the surface of the steel substrate. In contrast, the impedance value in low frequency of NR and low clay loading films was below 10^7, which indicates that the coating film was poor for the protection of CRS for this period of time.

Based on the results of sedimentation tests, the coating containing poorly dispersed organoclay (2I.30E), exhibited relatively weak corrosion protection performance on CRS. The effective enhancement of anticorrosion properties of 2CIP, as compared with those of 2I.30E and 1C coating systems, might have arisen from the well-dispersed silicate nanolayers of clay in an epoxy resin matrix. Such a behavior leads to more increase in the tortuosity of the diffusion pathway of the oxygen, water and ions. In other words, the relatively poor results of corrosion resistance of 2I.30E coating composition might be due to the presence of aggregates or agglomerates of tactoids in this composition.

Figure 7 also shows the same anticorrosion properties of 2CIP and 2C coating compositions. Based on sedimentation, XRD and TEM results, it seems that the 2CIP has a fully dispersed and exfoliated structure whereas 2C has only a well-dispersed structure. It could be concluded that the complete dispersion of clay layers in the matrix plays a more important role in corrosion resistance than exfoliation. However, even in exfoliated structures, careful consideration

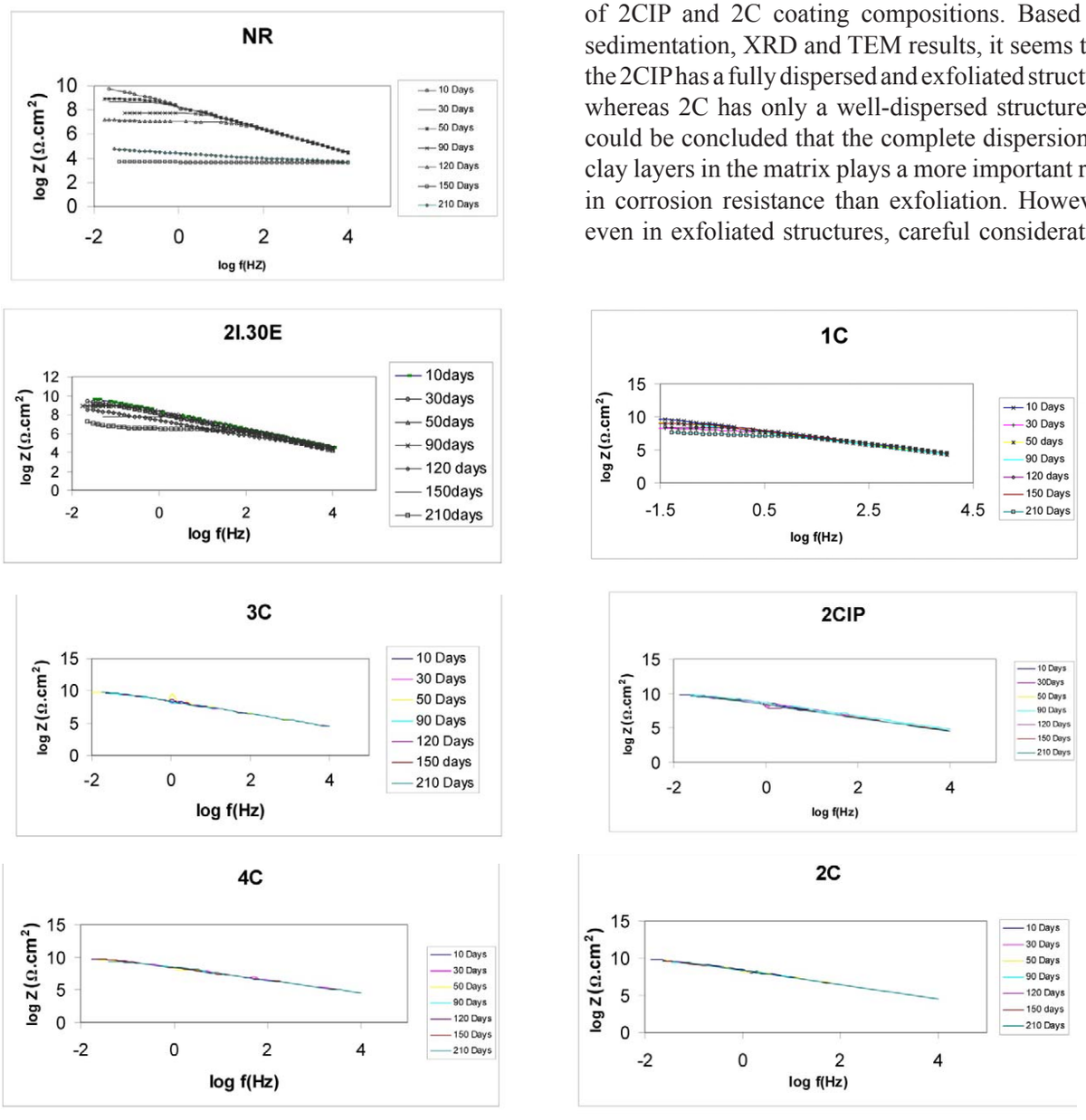

Figure 6: *EIS Bode plot of Coating Systems, NR, 1C, 2C , 3C, 2I.30E, 2CIP and 4C after different time of immersion in NaCl solution*

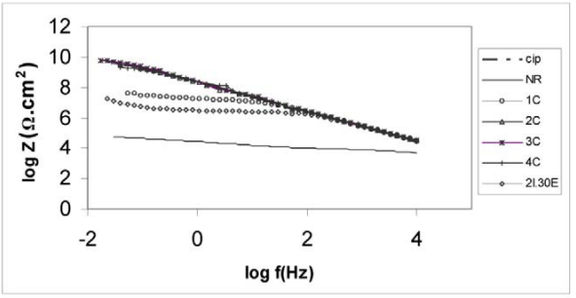

Figure 7: *Bode plot of NR, 1C, 2C, 3C, 4C, 2CIP, 2I.30E Coating Systems after 210 days of immersion*

of full dispersion of clay layers in the matrix and prohibition for the creation of aggregates is necessary. The compatibility of clay with the resin matrix and compounding method are two significant factors which determine the dispersion [23]. It must be noted that, even in exfoliated nanocomposite systems, there is a risk of incomplete exfoliation or inevitable aggregation of clay layers in the resultant nanocomposite. The presence of such clay aggregates in the microstructure of the nanocomposite has been previously reported by Kornmann et al**.** [34]. In the 2I.30E coating compositions, these clusters or aggregates of nanoparticles in the matrix might decrease the effective barrier surface of the layers and, as a result, the tortuous pathway of corrosive ions and corrosion resistance may also decreased. The high corrosion resistance of 2C and 2CIP imply that the efficiency of high-shear mixing plus sonication and the slurry methods are the same. It must be noted that the compatibility of modifier of organoclays with matrix is necessary.

As shown in Figures 6 and 7, the corrosion resistance of 2C, 3C and 4C were nearly the same and their corrosion resistivity was better than those of NR and 1C. It should be noted that a further increase in clay concentration in coating composition does not necessarily result in further enhancement of corrosion resistance in longer times of exposure to electrolyte. As a matter of fact, the rheological problems of the application of high-viscous coatings containing high clay loading, must be considered [23].

4. CONCLUSION

In this work, a set of nanocomposite coatings were prepared using epoxy resin and commercially modified MMt. The main factors which influenced the corrosion resistance were clay concentration, compatibility of clay modifier and quality of dispersion. The presence of clay in coating compositions led to superior anticorrosion properties compared with pure resin. Also, the coating composition containing raw clay modified with aminic hardener, via slurry compounding method, showed superior corrosion resistance. In well dispersed coating compositions, the best results were achieved with compositions containing two or more wt% of organoclay into the matrix. Poor dispersion of clay (caused by low compatibility of organoclay and matrix) led to poor corrosion resistance. It was revealed that, from corrosion resistance viewpoint, the impact of dispersion was greater than that of exfoliation of clay layers into the matrix. The present study confirmed the feasibility of developing new coating formulations from corrosion resistant epoxy-clay nanocomposite coatings with amine-modified or commercially modified clays without toxic inhibitors.

REFERENCES

1. D. W. Deberry, J. Electrochem. Soc. 132 (1985) 1022.
2. B. Wessling, Synth. Met. 41 (1991) 907.
3. W. K. Lu, R. L. Elsenbaumer, B. Wessling, Synth. Met. 71 (1995) 2163.
4. D. A. Wrobleski, B. C. Benicewicz, K. G. Thompson, C. J. Byran. Polym. Prepr. (Am. Chem. Soc, Div. Polym. Chem.) 35 (1994) 265.
5. B. Wessling, Adv. Mater. 6 (1994) 226.
6. W. Yen, W. Jianguo, J. Xinri, J. M. Yeh, P. Spellane, Polymer 36 (1995) 4535.
7. D. Zaarei, A. A. Sarabi, F. Sharif, S. M. Kassiriha, JCT RES. 5 (2008) 241.

8. EPA Federal Register, ‘‘National Emission Standards for Hazardous Air Pollutants for Source Categories: Aerospace Manufacturing and Rework Facilities 60 (1995) 45947.
9. A. Ramazan, O. C. Richard, Mat. Res. Soc. Symp. Proc., 2004, 788, L11. 44. 1.
10. C. Sanchez, G. J. De, A. A. Soler-Illia, F. Ribot, T. Lalot, C. R. Mayer, V. Cabuil, Chem. Mater. 13(2001) 306.
11. M. Ogawa, K. Kuroda. Bull, Chem. Soc. Jpn. 70(1997) 2593.
12. M. Alexandre, P. Dubois, Mater. Sci. Eng. R. Report. 28 (2000) 1–63.
13. Y. C. Ke, P. Strove, Polymer Layered Silicate, Silica Nanocomposites. Elsevier, Amsterdam, 2005.
14. E. Ruiz-Hitzky, Chem. Rec. 3(2003) 88.
15. E. Ruiz-Hitzky, Nanostructured, Functional Hybrid Materials. In: P. Go´ mez-Romero, C. Sa´nchez (eds.) Functional Hybrid Materials, p. 15. Wiley-VCH, Weinheim,2004.
16. J. M. Yeh, H. Y. Huang, C. L. Chen, W. F. Su, Y. H. Yu, Surf. Coat. Tech. 200 (2006) 2753.
17. K. Wang, L. Wang, J. Wu, L. Chen, C. He, Langmuir. 21(2005) 3613.
18. K. Wang, L. Chen, J. Wu, M. L. Toh, C. He, A. F. Yee, Macromolecules 38(2005) 788.
19. L. Wang, K. Wang, L. Chen, C. He, Y. Zhang, Polym. Eng. Sci. 46(4006)215.
20. Lit. G-105 Revised 05/05/06, Polymer grade montmorillonite. Product Sheet (3-29-04), Nanocor, Inc., Arlington Heights, IL. 2004.
21. W. Liu, S.V. Hoa, M. Pugh, Comp. Sci. Tech. 65 (2005) 307.
22. J. Ma, Z.Z. Yu, Q. Zhang, X. L. Xie, Y. W. Mai, I. Luck, Chem. Mater. 16 (2005) 757.
23. D. Zaarei, A. A. Sarabi, F. Sharif, S. M. Kassiriha, M. Moazzami Gudarzi, e-Polymers 117(2008)1.
24. L. Chen, K. Wang, M. L. Toh, C. He, Macromolecular Materials and Engineering 290(2005) 1029.
25. J. H. Park, S. C. Jana, Macromolecules 36(2003) 2758.
26. W. J. Boo, L. Sun, J. Liu, E. Moghbelli, A. Clearfield, H.J. Sue, H. Pham, N. Verghese, J. Polym. Sci. Part B: Polym. Phys. 45(2007) 1459.
27. S. Lingaiah, K. N. Shivakumar, R. Sadler, M. Sharpe,Comp. Sci. Tech. 65(2005) 2276.
28. J. Park, S. C. Jana, Macromolecules 36(2003) 8391.
29. B. Xu, Q. Zheng, Y. Song, Y. Shangguan, Polymer 47(2006) 2904.
30. L. Beaunier, I. Epelboin, J. C. Lestrade, H. Takenouti, Surf. Technol. 4 (1976) 237.
31. N. Pébère, T. Picaud, M. Duprat, F. Dabosi, Corros. Sci. 29(1989) l073.
32. A. Kalendova, Prog. Org. Coat. 46 (2003) 324.
33. H. Shi, F. Liu, E. Han, Y. Wei, J. Mater. Sci. Techno. 23(2007) 551.
34. X. Kornmann, H. Lindberg, L. A. Berglund, Polymer 42 (2001) 1303.

Aims and Scope

International Journal of Nanoscience and Nanotechnology IJNN; is published by the Iranian Nanotechnology Society INS. The Journal publishes original scientific research papers in a broad area of nanotechnology.

Instructions to Authors

Submission of Manuscript

The language of the journal is English. Papers should deal with original research not previously published or sent for publication elsewhere.

Manuscripts should be submitted online through the site: **www.ijnnonline.net.** They should include all illustrations, photographs, drawings, tables etc. The manuscript is expected to be qualified for peer review by using the format and style of the journal with a good standard English. Manuscripts that have not fulfilled such requirements will be rejected. During the review process, the status of manuscripts could be followed either through the site or via the address below:

Editorial Office IJNN;
Unit 8, 3th Floor, No. 10, Javahery Street,
Karegar Shomali Street, Tehran, I. R. Iran
Tel: +98-21-6690-1553, Fax:+98-21-6659-4061
Email: ipro@nanosociety-ir.com

Types of Articles

Articles will be published in the following categories:

1- Full Research Papers: They expect to be preferably subdivided into seven sections; namely as Abstract, Introduction, Materials and Methods, Experimental Results, Discussion and Conclusion, Acknowledgment and References.

2- Short communications: They include short scientific notes, such as useful methods with special application in Nanotechnology. Brief extensions of previously published work may also be submitted for publication as short communications. These should not exceed 6 typed pages with a short abstract of a maximum 100 words. The text should be continuous and not be subdivided in different sections as a regular paper.

3- Reviews: Reviews in Nanotechnology that organize and/or summarize a research literature relevant to the aforementioned topics can be accepted. Review articles are invited from leading researchers who are well known in a subject area of nanotechnology. The first requirement for accepting a review article is that the corresponding author must have at least 3 research articles quoted in the reference list of the paper. Reviews should objectively chronicle recent and important developments. A full review paper is limited to 25 typed pages including Tables and figures. All the Review articles are subject to peer review.

Manuscript Organization

Manuscript should be written in English and clearly typed (font size 11 Points, Times New Roman) and double-spaced throughout with 2.5 cm margins. All pages should be consecutively numbered.

Title page: In addition to a brief, descriptive, concise title of the article, the full name of the author(s), academic or professional affiliation and addresses should be included on the title page. The name and